Measurement of through-plane effective thermal conductivity and contact resistance in PEM fuel cell diffusion media

G. Karimi [1], X. Li [*], P. Teertstra

Department of Mechanical and Mechatronics Engineering, University of Waterloo, 200 University Avenue West, Waterloo, Ontario N2L 3G1, Canada

ABSTRACT

An experimental study was performed to determine the through-plane thermal conductivity of various gas diffusion layer materials and thermal contact resistance between the gas diffusion layer (GDL) materials and an electrolytic iron surface as a function of compression load and PTFE content at 70 °C. The effective thermal conductivity of commercially available SpectraCarb untreated GDL was found to vary from 0.26 to 0.7 W/(m °C) as the compression load was increased from 0.7 to 13.8 bar. The contact resistance was reduced from 2.4×10^{-4} m²°C/W at 0.7 bar to 0.6×10^{-4} m²°C/W at 13.8 bar. The PTFE coating seemed to enhance the effective thermal conductivity at low compression loads and degrade effective thermal conductivity at higher compression loads. The presence of microporous layer and PTFE on SolviCore diffusion material reduced the effective thermal conductivity and increased thermal contact resistance as compared with the pure carbon fibers. The effective thermal conductivity was measured to be 0.25 W/(m °C) and 0.52 W/(m °C) at 70 °C, respectively at 0.7 and 13.8 bar for 30%-coated SolviCore GDL with microporous layer. The corresponding thermal contact resistance reduced from 3.6×10^{-4} m²°C/W at 0.7 bar to 0.9×10^{-4} m²°C/W at 13.8 bar. All GDL materials studied showed non-linear deformation under compression loads. The thermal properties characterized should be useful to help modelers accurately predict the temperature distribution in a fuel cell.

© 2009 Elsevier Ltd. All rights reserved.

1. Introduction

Detailed knowledge of in situ temperature distribution in a polymer electrolyte membrane (PEM) fuel cell is essential for better understanding of the thermal and water transport in a PEM fuel cell and optimization of cell performance. Direct internal temperature measurements introduce major challenges due to the minute length scale involved, anisotropic nature of porous media, and existence of complex two-phase flow in the PEM fuel cell. Although various modeling approaches [1–4] have been presented based on simplified geometric and modeling properties to predict the temperature distribution in PEM fuel cells under different operating conditions, the modeled results may not reflect the actual phenomena occurring in the fuel cell due to limited information on the thermo-physical properties, in particular, thermal conductivity and thermal contact resistance of various fuel cell components.

A literature review shows that thermal conductivity of the most commonly used membrane, Nafion®, is well known [5]. However, the thermal conductivity and contact resistance of diffusion media or gas diffusion layers (GDLs) are more difficult to estimate. The

porosity of the GDLs makes it necessary to use effective thermal conductivities to describe heat transfer in the solid and fluid phases [6]. In addition to having high porosities, the GDL materials are also anisotropic, which is probably the reason why thermal conductivity values in literature are so dispersed widely as illustrated in Table 1.

As indicated, most of the results reported in Table 1 are estimated from the thermal conductivities of each phase and their volumetric fraction in the medium. Even the experimentally measured values show significant dispersion. In this study, experimental measurements have been conducted for the thermal characteristics of diffusion media in PEM fuel cells.

There are in principal two classes of methods to measure a thermal conductivity and/or thermal contact properties. In the first class, referred to as transient methods, the temperature is recorded with respect to time and position when the surrounding temperature suddenly changes. The information about the heat capacity of the investigated material is required in this method. The laser-flash radiometry technique [20] is an example of a transient method, which may be applied at elevated temperatures. The second class of methods involves a known, controlled heat flux and measures temperatures at different locations through the sample [21].

Thermal properties of diffusion media are difficult to investigate by the transient method due to the size, material structure and barely known heat capacities. Therefore, transient methods

---

* Corresponding author.
E-mail address: x6li@uwaterloo.ca (X. Li).
[1] On leave from Shiraz University, Shiraz, Iran. E-mail: ghkarimi@shirazu.ac.ir.

are usually considered incomprehensive for obtaining thermal conductivities of diffusion media. In situ measurements of thermal properties in PEM fuel cells are also challenging due to the minute length scale and the complexity of the numerous processes taking place during cell operation. More accurate thermal conductivity values of GDL materials and their thermal contact resistances can be determined ex situ using heat flux meters.

As listed in Table 1, several studies have been performed by various researchers to determine thermal properties of GDL materials with and without the compression load. Burford and Mench [16] estimated thermal conductivity of diffusion media and Nafion® by measuring electrolyte temperature using micro-thermocouples embedded in the electrolyte. Ihonen [15] reported the thermal impedance of a 100 μm Sigracet® PTL as a function of applied pressure. The reported thermal conductivity varied between 0.05 and 0.125 W/(m °C) as the compression loads change from 1 to 8 bar. No variances in these values were provided. Vie and Kjelstrup [17] calculated thermal conductivities from measured temperature profiles across the membrane inside a single PEM fuel cell. They reported an average thermal conductivity of 0.2 ± 0.1 W/(m °C) for the catalyst layer plus GDL.

Few experimental studies have been carried out for contact resistance between GDLs and other fuel cell components. The contact resistance has been typically estimated roughly or simply overlooked in modeling studies [22,23,5]. This parameter, however, may be a key factor to determine the current and temperature distribution inside the cell and needs to be investigated in sufficient detail for the following reasons: (a) the contact resistance value can be substantially large, (b) significant variation in the contact resistance values over the cell area can exist because of the rib/channel structure of the neighboring bipolar plate, and (c) the compression pressure could have significant effects on the thermal contact resistance of GDL materials with different surfaces.

Khandelwal and Mench [18] measured the thermal conductivity of diffusion media as a function of polytetrafluoroethylene (PTFE) content, temperature and compression loads using heat flux meter. They reported thermal conductivity of 0.22 ± 0.04 W/(m °C) for SIGRACET® diffusion media treated with 20 wt% PTFE. This value doubled in the absence of PTFE. Toray diffusion media were found to have a thermal conductivity of 1.80 ± 0.27 W/(m °C) at 26 °C. They assumed that the bulk conductivity and sample thickness remain constant with applied pressure. Ramousse et al. [5] reported an effective thermal conductivity for the gas diffusion layers provided by Quintech and SGL Carbon. Neglecting the contact

resistances, minimum through-plane thermal conductivities were ranged from 0.20 to 0.36 W/(m °C) for Quintech diffusion media (230, 280, 190 μm, respectively) and 0.260 W/(m °C) for the SGL Carbon (420 μm).

Recently, Burheim et al. [19] demonstrated an experimental methodology to determine the thermal conductivity of deformable diffusion materials as a function of compaction pressure. The thermal conductivity and the thermal contact resistance to an aluminium plate for an uncoated SolviCore GDL were determined at various compaction pressures. For dry GDL at 4.6, 9.3 and 13.9 bar compaction pressure, the thermal conductivity was found to be 0.27, 0.36 and 0.40 W/(m °C), respectively, and the thermal contact resistivity to the apparatus was determined to be 2.1, 1.8 and 1.1×10^{-4} m² °C/W, respectively. It was shown that the thermal contact resistance between two GDLs is negligible compared to the apparatus contact resistivity.

The literature review on thermal characteristics of diffusion media has clearly indicated that the performance of PEM fuel cells is highly dependent on the type of GDL and its behavior under various operating conditions. Specifically, the PTFE content of diffusion media, the clamping pressure (load) under which various cell components are assembled and the cell operating temperature are very important. To this end, the objective of this paper is to present an ex situ experimental method to measure the through-plane effective thermal conductivity and thermal contact resistance of different GDL materials as a function of the amount of PTFE content and compression load. It is believed that the experimental results reported in this paper will add to the PEM fuel cell knowledge base and provide reliable bench mark data for modelers to accurately predict the temperature distribution in a fuel cell.

2. Materials and methods

2.1. Structure

Diffusion media used in PEM fuel cells are made from either carbon fiber paper or carbon cloth. Two kinds of commercially available carbon paper GDLs were used in this study; SpectraCarb pure carbon paper GDL ($t = 190$ μm) and SolviCore carbon paper with 30% PTFE content and microporous layer (MPL) on one side ($t = 250$ μm). The SpectraCarb carbon paper was also coated in-house with 12, 19 and 29 wt%. PTFE in order to examine the effect of PTFE content on its thermal behavior. The surface roughness profiles of the materials were observed using an optical profiler to measure the average surface roughness. The 3D roughness profiles for the samples are depicted respectively in Fig. 1a–c for the different surfaces. From the measurements, the SpectraCarb pure GDL shows the largest surface roughness ($\sigma = 18.71$ μm) and the MPL side of the SolviCore paper shows the smallest surface roughness ($\sigma = 6.40$ μm). The difference in the GDL material and surface conditions imply variations in the GDL effective thermal conductivity as well as the thermal contact resistance.

2.2. Test apparatus

All thermal property measurements were performed using a thermal conductivity test apparatus, with its design based on the guarded heat flux meter device recommended by the ASTM standard [24] with a number of modifications. The test column in the apparatus shown in Fig. 2 was comprised of two calibrated electrolytic iron flux meters with a 25 mm × 25 mm cross sectional area. Temperatures were measured at 10 mm intervals along each of the flux meters using five 1-mm dia. × 25 mm ceramic resistance temperature detectors (RTD). A heater block with four embedded cartridge heaters was positioned at the bottom of the test column

Table 1
Reported effective thermal conductivities of diffusion media.

Author/reference	k [W/(m °C)]
Estimation	
Maggio et al. [7]	15.56
Wohr et al. [8]	65
Gurau et al. [9]	21.5
Argyropoulos et al. [10]	0.15
Toray Industries Inc. [11]	1.6
Rowe and Li [12], Djilali and Lu [13]	1.6
Nguyen et al. [14]	1.3
Ju et al. [1]	0.5; 1; 2.94
Hwang [3]	1.7
Measurements	
Ihonen [15]	0.05–0.125
Burford and Mench [16]	0.13–0.19
Vie and Kjelstrup [17]	0.2 ± 0.1
Khandelwal and Mench [18]	1.24 ± 0.19 at 73 °C
	1.8 ± 0.27 at 26 °C
Ramousse et al. [5]	0.20–0.36 and 0.3–1.36
Burheim et al. [19]	0.27–0.4
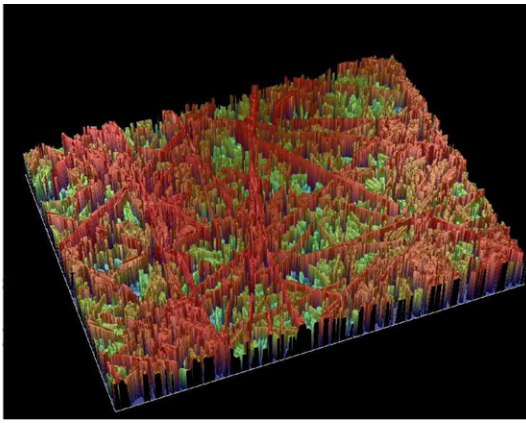
(a) SpectraCarb pure carbon paper GDL ($\sigma = 18.71 \mu$m)
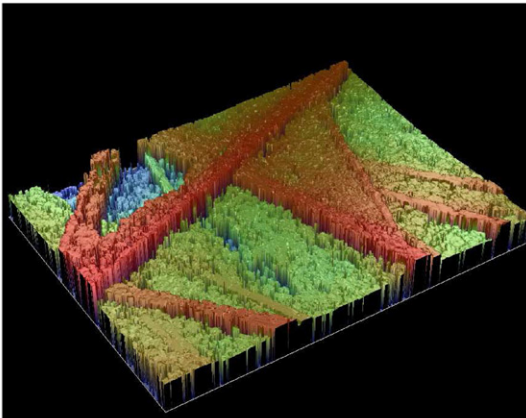
(b) SolviCore carbon paper GDL with 30% PTFE ($\sigma = 15.80 \mu$m)
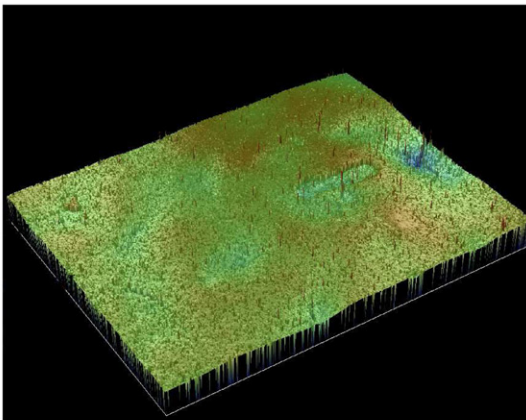
(c) MPL side of SolviCore carbon paper GDL ($\sigma = 6.40 \mu$m)

Fig. 1. Surface characteristics of the test samples as imaged by surface profilometer. (a) SpectraCarb pure carbon paper GDL ($\sigma = 18.71\,\mu$m); (b) SolviCore carbon paper GDL with 30% PTFE ($\sigma = 15.80\,\mu$m); (c) MPL side of SolviCore carbon paper GDL ($\sigma = 6.40\,\mu$m).

while the temperature of the cold plate at the top of the column was regulated using a glycol–water solution from a constant temperature bath. The test samples were placed between the lapped upper and lower surfaces and the contact pressure at the interface between the flux meters was measured using a load cell which was adjusted using a linear actuator. All measurements were performed using a Keithley 2700 data acquisition system controlled with Labview program running on a desktop PC. A full description of the apparatus and details of its construction and operation were presented by Culham et al. [25].

The primary objective of this study is to examine the thermal conductivity and contact resistance of diffusion media over a wide range of compression loads. Therefore, it is extremely important to ensure that the applied loads are uniform. The uniformity of the pressure distribution across the contacting surfaces of the heat flux meters was verified using Pressurex [26] ultralow pressure indicating film (1.7–5.7 bar). Further, it is expected that the in situ materials thickness to vary due to external loading and thermal expansion. Therefore, a precise measurement of the materials thickness was essential. In the present study, a laser-based system was used for in situ thickness measurements with a resolution of 2 μm.

2.3. Test procedure

The procedure used for measurement of the joint resistance between the flux meter surfaces contacting the sample was as follows. The square sample ($S = 6.25 \times 10^{-4}\,\text{m}^2$) was placed between the flux meters and a small preliminary load was applied to align the test column and the data acquisition software was started. The desired set of compression loads and joint temperature were specified. The measurements started at low compression loads and proceeded to higher pressures. The contact pressure, temperature distributions, the lower and upper heat fluxes and the sample thickness were all monitored using the data acquisition system. Once the desired contact pressure and sample temperature were achieved and a steady-state condition was reached, the temperatures of the RTDs and the sample thickness were recorded.

2.4. Data analysis and interpolation

A typical RTD temperatures plotted vs. position in the flux meter is shown in Fig. 3. The total heat flow rate through each of the flux meters is calculated by

$$Q = k(T)S\frac{dT}{dx} \tag{1}$$
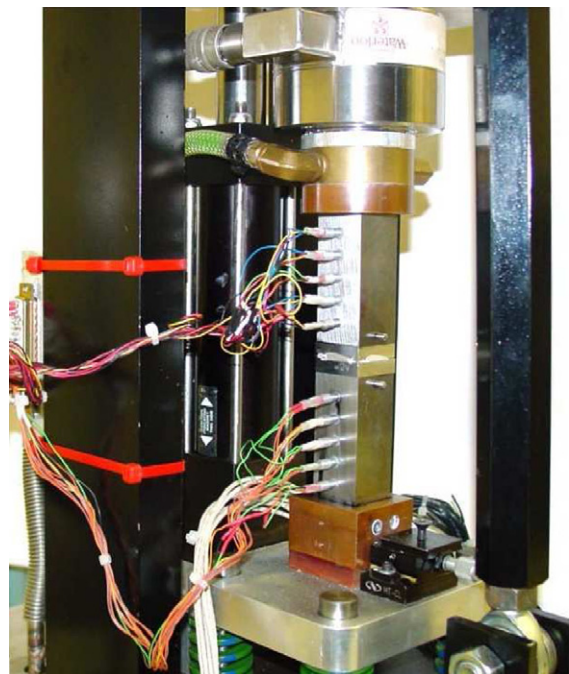
Fig. 2. Experimental setup for thermal conductivity and thermal contact resistance measurements.
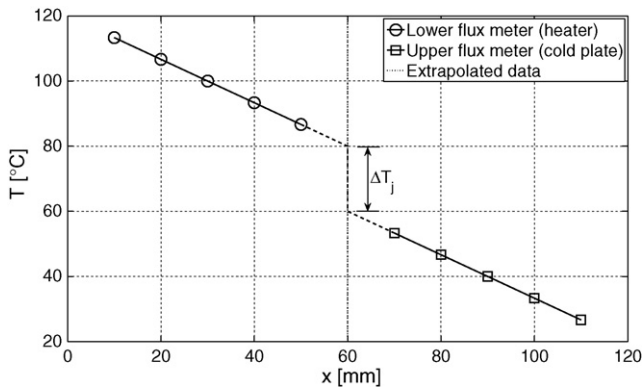
Fig. 3. A typical heat flux meter temperature distribution.

where $k(T)$ is the thermal conductivity of the calibrated flux meter material, correlated with respect to average temperature, S is the cross sectional area (6.25×10^{-4} m^2), and dT/dx is the temperature gradient, calculated using a linear least squares fit of the data as illustrated in Fig. 3. Due to the radial heat leakage, the total heat flow rate calculated for the lower and upper flux meters differed slightly for all cases (see Section 2.5 for details), therefore, the mean value of the heat fluxes was used in the analysis.

The total joint thermal resistance, R_t, is determined as

$$R_t = \frac{\Delta T_j}{Q_{ave}} \tag{2}$$

where Q_{ave} is the mean value from the upper and lower heat flux meters and ΔT_j is the temperature difference at the joint, calculated based on an extrapolation of the least squares fit of the data to the contacting surfaces of the flux meters, as shown in Fig. 3.

The measured thermal resistance at the joint, R_t, is the sum of the sample thermal resistance, R_m, and the contact resistances between the sample and the metallic surfaces, R_{co}, so that:

$$R_t = R_m + 2R_{co} \tag{3}$$

As indicated in Eq. (4), although the thermal resistance of the sample is a function of its effective thermal conductivity, k_m, and thickness, the sample-to-metal contact resistance is a complex function of thermal conductivities, contact pressure and surface characteristics such as surface roughness, asperity, and the sample microhardness [27]:

$$R_m = \frac{t(P)}{k_m S} \quad \text{and} \quad R_{co} = f(k_m, \ k_{iron}, \ P, \ \text{surface properties}) \tag{4}$$

The measurement of thermal characteristics of GDL samples becomes significantly complicated by the fact that these porous materials deform under load and as a result, the bulk thermal conductivity changes. Therefore, it is not possible to separate the contact resistance from the bulk conductivity by simply varying the pressure. In addition, GDL materials are not typically available in different thicknesses, or if they are it is expected that the porous structure varies with the material thickness [5]. An alternative approach is to vary the thickness by stacking different numbers of individual samples. This however introduces a new variable, the contact resistance between individual samples. Theoretically, a stack of up to three identical samples would be required to form a closed set of three equations and three unknowns. In this case, total thermal resistance, R_t, can be expressed as

$$R_{t,n} = nR_m + (n-1)R_{ci} + 2R_{co} \quad n = 1, 2, 3 \tag{5}$$

The increase in the total resistance with the number of layers corresponds to the sum of material resistance, R_m, and extra contact resistance between layers, R_{ci}. It seems from Eq. (5) that if a series of experiments are performed using a single, two and three sample layers, then the three unknowns R_m, R_{ci} and R_{co} can be determined. However, a thorough examination of the set of the equations reveals that a unique solution does not exist. The layer-to-layer thermal contact resistance was shown to be negligible [19] compared to the medium-to-metallic surface. Therefore, R_{ci} can be omitted from the set (Eq. (5)) and experiments with only one and two sample layers would be sufficient. Under such conditions, Eq. (5) is reduced to

$$R_{t,n} = nR_m + 2R_{co} = \frac{t_n}{k_m S} + 2R_{co} \quad n = 1, 2 \tag{6}$$

where t_n is the sample thickness corresponding to n layers. Neglecting the inner contact resistances (R_{ci}), would result in thermal conductivity values which are more conservative. According to Eq. (6), the effective thermal conductivity of the material and the associated thermal contact resistance can be determined using a linear fit of $R_{co,n}$ vs. t_n for single and double material layers as indicated in Eqs. (7) and (8).
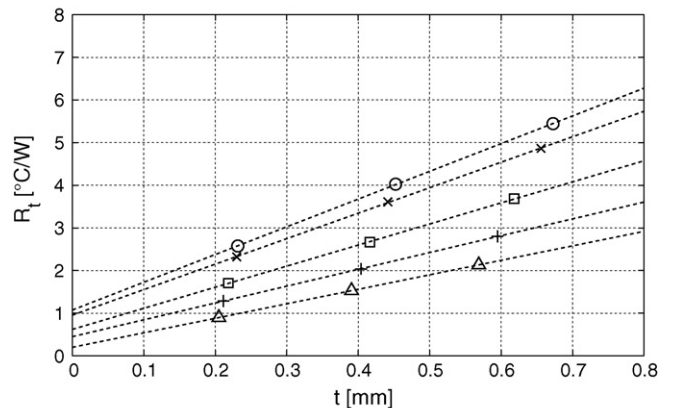
$$k_m = \frac{1}{\text{slope} \times S} \tag{7}$$

$$R_{co} = \frac{1}{2} \times \text{intercept} \tag{8}$$

For a larger number of material layers (e.g. $n = 3$ used in the present study), a least square fit of the data will provide more precise results. This procedure is illustrated in Fig. 4 for three layers of SpectraCarb pure GDL at 1.33 bar compression load.
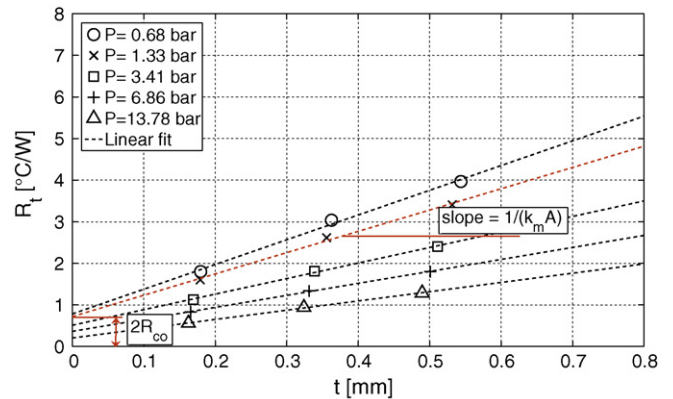
(a) SpectraCarb pure GDL

(b) SolviCore PTFE-coated GDL with MPL

Fig. 4. Total thermal resistances, R_t, as a function of applied load, P, for single, double and three-layer samples, represented by the left, middle and right data points on each curve in the figure. (a) SpectraCarb pure GDL; (b) SolviCore PTFE-coated GDL with MPL.

2.5. Uncertainty analysis

The uncertainty in the total resistance measurements of the test apparatus can be calculated based on the combined uncertainties inherent in the temperature drop at the interface and heat flow rate calculations, as reported by Savija et al. [28]. The uncertainty in the linear fit of the five RTD temperature readings is estimated at 0.1 °C, which leads to an uncertainty of 0.2 °C for the temperature drop across the joint. The uncertainty in the heat flow rate, Q, results from two main sources; the uncertainty in the temperature gradient calculated using a least squares linear fit of the RTD temperature measurements and estimated as 0.5%, and the difference in the heat flow rates between the two flux meters due to heat loss to the surroundings. Since the mean of these two readings is used to calculate resistance, one half of the percent difference between the upper and lower flux meters represents a good estimate of the uncertainty in Q_{ave}.

Combining the uncertainties using the method described by Moffat [29], the uncertainty in the thermal resistance is calculated by

$$\frac{\delta R_t}{R_t} = \left[\left(\frac{\delta \Delta T}{\Delta T} \right)^2 + \left(\frac{\delta Q}{Q} \right)^2 \right]^{1/2} \quad (9)$$

$$\frac{\delta R_t}{R_t} = \left[\left(\frac{0.2}{\Delta T \ [^\circ C]} \right)^2 + (0.005)^2 + \left(\frac{1}{2} \frac{Q_{hot} - Q_{cold}}{Q_{ave}} \right)^2 \right]^{1/2} \quad (10)$$

The uncertainty values for the present experiments range from a maximum of 12.9% for three layers of pure GDL at the lowest value of contact pressure, where the difference between the flux meter values was the largest, to a minimum of 4.9% for a single layer of the same material at the highest contact pressure.

The contact pressure is calculated based on force measurements performed using a Sensotec 4450 N load cell with an uncertainty of 0.1% of full scale, or $\delta F = 4.5$ N. The contact area is affected by the alignment of the upper and lower flux meters when the sample is placed in the test apparatus. Since this alignment is done visually and by hand, the uncertainty is estimated as 0.5 mm per 25 mm side.

The uncertainties in the force measurement and the sample alignment were combined to calculate the uncertainty in the calculated value of the contact pressure.

$$\frac{\delta P}{P} = \left[\left(\frac{\delta F}{F} \right)^2 + \left(2\frac{\delta L}{L} \right)^2 \right]^{1/2} = \left[\left(\frac{4.5}{F \ [N]} \right)^2 + \left(\frac{1}{25} \right)^2 \right]^{1/2} \quad (11)$$

The uncertainty values in contact pressure measurements vary between 4 and 11% for the range of loads measured in this study.

The effective thermal conductivity of the material is calculated using a linear, least squares fit of the data for single and multiple material layers at a fixed value of contact pressure. The uncertainty in the thickness measured by the Laser Scan Micrometer is $\delta t = 0.3\%$, significantly smaller than the uncertainty calculated for the resistance values and may therefore be neglected. Therefore the uncertainties in the calculated values of thermal conductivity are the same as those of the thermal resistance.

3. Results and discussions

Experiments were performed to measure the effective thermal conductivity and thermal contact resistance of two diffusion materials commonly used in PEM fuel cell applications. The materials studied were SpectraCarb carbon paper GDL with 0, 12, 19 and 29 wt%. PTFE contents and SolviCore carbon paper GDL with 30 wt%. PTFE content and MPL. All experiments were conducted at a mean

joint temperature of 70 °C and under a wide range of compression loads.

Diffusion media deform when subjected to compression loads. Therefore, the accuracy of the measured thermal conductivity and contact resistances depends strongly on the precision of the thickness measurement. This has been neglected in some previous studies (e.g. [5]). A relative compression, RC, can be defined to evaluate sample deformations under compression loads:

$$RC = 100 \left[1 - \frac{t_0 - t_P}{t_0} \right] \quad (12)$$

where t_0 and t_P are the thickness of the material subjected to no load and a compression load of P, respectively. Fig. 5 shows how different GDL materials perform under compression loads. As indicated, all diffusion materials deform non-linearly with the compression loads. However, the SpectraCarb pure GDL and its variants show less deformation than the SolviCore GDL. The initial rate of deformation for all GDL materials is high but decreases as the compression load is increased. The present data indicate the existence of an asymptote corresponding to a compression load of about 20 bar (not shown in the figure). The CR values shown in Fig. 5 indicated respectively 16% and 22% thickness reductions in SpectraCarb and SolviCore GDLs when the applied load increased from 0 to 14 bar. The RC observed in this work is two times larger than the value reported recently by Burheim et al. [19] for SolviCore GDL. In addition, the non-linear RC-load relation appears in Fig. 5 seems to be more realistic than the linear behavior reported by Burheim et al. [19].

Variations of total thermal resistances R_{co} as a function of applied load for single, double and three-layer stacks of SpectraCarb pure GDL and PTFE-coated SolviCore GDL with MPL materials are shown respectively in Fig. 4a and b. As expected, R_{co} increases linearly with the number of layers (thickness) at the same compression load and decreases as the applied load is increased. As shown in these figures, the R_{co} values for PTFE-coated SolviCore GDL material is larger than that of the untreated GDL. This is possibly due to the coverage of some of the high thermal conductive carbon fibers ($k_{carbon} = 129$ W/(m °C) [30] by low thermally conducting PTFE material ($k_{PTFE} = 11.7$ W/(m °C) [31].

In the absence of layer-to-layer thermal contact resistance, the effective thermal conductivities and thermal contact resistances can be obtained from Eqs. (7) and (8). Fig. 6a and b shows how the thermal contact and medium resistances vary with the applied compression loads for different media. As expected, all resistances are decreased with the applied pressures. It is observed from Fig. 6a that both PTFE-coated SpectraCarb and SolviCore GDLs present larger thermal contact resistances than the untreated SpectraCarb GDL at all pressures. This is primarily due to the PTFE coating on GDL
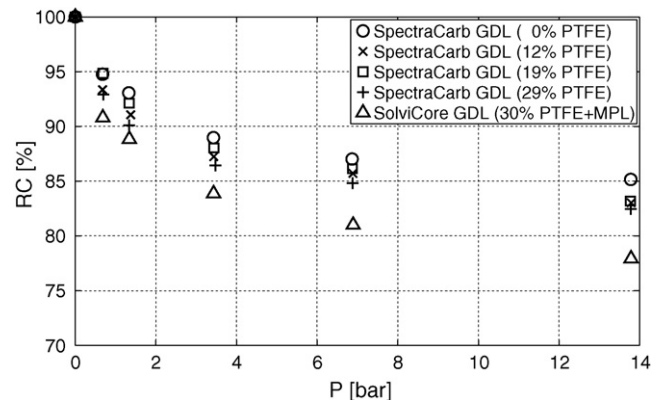
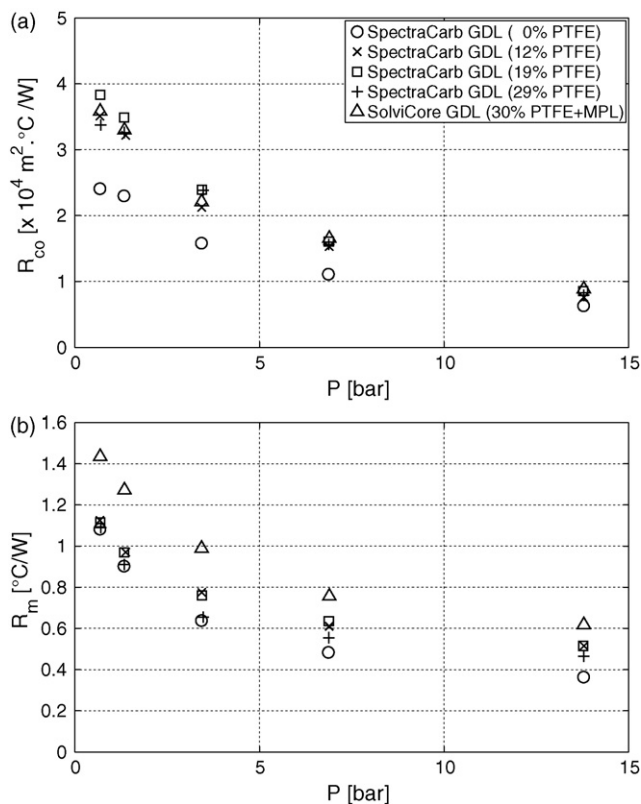**Fig. 5.** Relative compression of various GDLs as a function of applied load.

Fig. 6. Comparison of (a) thermal contact resistances, R_{co}, and (b) effective thermal resistances, R_m, of the diffusion media at different compression loads.

surfaces in contact with the electrolytic iron surface. Fig. 6b compares the effective thermal resistance associated with the different materials. As indicated, the untreated SpectraCarb GDL presents lower thermal resistance than all of its PTFE-coated variants and the PTFE-coated SolviCore material. However, the effective thermal conductivity must be determined based on the actual thickness of the materials.

Fig. 7 shows the effective thermal conductivity of different GDLs as a function of the compression load. As displayed in the figure, the PTFE-coated SolviCore GDL presents the lowest thermal conductivity under all compression loads. However, the thermal behavior of SpectraCarb GDL materials was slightly different. At low compression loads, the thermal conductivity of the GDL was enhanced in the presence of PTFE while the untreated GDL shows superior conductivity at higher pressure loads.
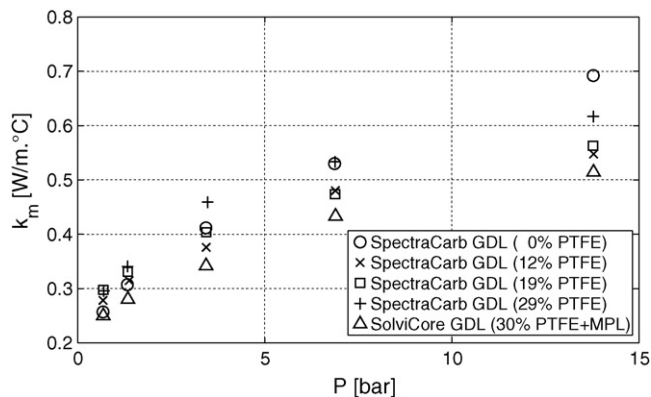

Fig. 7. Measured effective thermal conductivities of the various diffusion media as a function of compression load.

The different thermal behavior observed from both materials can be explained as follows. In general, thermal characteristics of diffusion media used in PEM fuel cells depend on the following key factors: (a) the material structure (the main characterizing parameter often used is the medium porosity), and (b) PTFE content. Both the effective thermal resistance of the diffusion media and thermal contact resistances are expected to amplify with increasing porosity. As shown earlier in Fig. 1, both surfaces of the SolviCore GDL were smoother than the surfaces of SpectraCarb untreated GDL (6.4, 15.8 μm vs. 18.60 μm). As a result, SolviCore GDL should offer a better contact with the iron surface. However, experimental data shows otherwise. This is because PTFE coating ($k_{PTFE} = 11.7\,W/(m\,°C)$) on the SolviCore GDL surfaces imposes a more significant impact on the surface contact resistances than the surface roughness. The measured thermal contact resistances for SolviCore treated GDL and SpectraCarb untreated GDL with iron surfaces ranged respectively from 3.6×10^{-4} to $8.8 \times 10^{-5}\,m^2\,°C/W$ and 2.4×10^{-4} to $6.3 \times 10^{-5}\,m^2\,°C/W$ as the compression pressure was varied from 0 to 14 bar. The PTFE coatings (12%, 19% and 29%) on the SpectraCarb GDLs increased the thermal contact resistance as well. The measured contact resistances may be different from the contact resistance with graphite or other cell materials with different surface finish. The variations in the thermal conductivity of the variants of SpectraCarb GDLs can be attributed to the presence of PTFE in GDL pores which control its thermal conductivity at lower compression loads.

4. Conclusions

An experimental technique was used to determine the effective through-plane thermal conductivity and contact resistance of different type of GDL materials under steady-state conditions. The following conclusions can be made regarding this work: (a) The experimentally measured thermal conductivity for SpectraCarb untreated GDL varied from 0.26 to 0.7 W/(m °C) when the compression load was increased from 0.7 to 13.8 bar at 70 °C. The thermal contact resistance for this material with smooth iron surface was estimated as $2.4 \times 10^{-4}\,m^2\,°C/W$ at 0.7 bar and $0.6 \times 10^{-4}\,m^2\,°C/W$ at 13.8 bar. (b) The effective thermal conductivity of PTFE-treated SpectraCarb diffusion material slightly increased at low compression loads and slightly decreased at higher compression loads. (c) The presence of the microporous layer (MPL) on SolviCore carbon fiber caused the effective thermal conductivity and contact resistance to decrease with respect to untreated GDLs. (d) The GDL materials used in the present study deformed non-linearly with the applied load. A maximum of 22% deformation was observed for 30%-coated SolviCore GDL with MPL when exposed to a compression load of 13.8 bar. (e) The effective thermal conductivities increased and the thermal contact resistances decreased with the applied load for GDL materials studied.

Acknowledgements

Appendix A. Nomenclature

d	differential
F	force [N]
L	length [m]

k	thermal conductivity [W/(m °C)]
n	number of sample layers
P	load/pressure [psi]
Q	heat flow rate [W]
R	thermal resistance [m^2 °C/W]
RC	relative compression [%]
S	sample area [m^2]
t	sample thickness [m]
T	temperature [°C]
x	distance [m]

Greek letters

δ	difference
Δ	difference
σ	roughness [m]

Subscripts

0	zero load
avg	average
carbon	carbon fiber
ci	contact-inner
co	contact-outer
cold	cold surface
hot	hot surface
j	joint
iron	electrolytic iron
m	medium
n	number of sample layers
t	total
P	pressure
PTFE	poly tetra fluoro ethylene

References

[1] H. Ju, H. Meng, C.Y. Wang, Int. J. Heat Mass Transfer 48 (2005) 1303.
[2] T. Berning, D.M. Lu, N. Djilali, J. Power Sources 106 (2002) 284.
[3] J.J. Hwang, J. Electrochem. Soc. 153 (2) (2006) 216.
[4] E. Birgersson, M. Noponen, M. Vynnycky, J. Electrochem. Soc. 152 (5) (2005) 1021.
[5] J. Ramousse, S. Didierjean, O. Lottin, D. Maillet, Int. J. Therm. Sci. 47 (2008) 1.
[6] C. Moyne, S. Didierjean, H.P. Amaral Souto, O.T. da Silveira, Int. J. Heat Mass Transfer 43 (2000) 3853.
[7] G. Maggio, V. Recupero, C. Mantegazza, J. Power Sources 62 (1996) 167.
[8] M. Wohr, K. Bolwin, W. Schnurnberger, M. Fischer, W. Neubrand, G. Eigen-berger, Int. J. Hydrogen Energy 23 (3) (1998) 213.
[9] V. Gurau, H. Liu, S. Kaka, AIChE J. 44 (11) (1998) 2410.
[10] P. Argyropoulos, K. Scott, W.M. Taama, J. Power Sources 79 (1999) 169.
[11] Toray Industries Inc., Toray Carbon Paper, Toray Industries Inc., Advanced Composites Department, 2001.
[12] A. Rowe, X. Li, J. Power Sources 102 (12) (2001) 82.
[13] N. Djilali, D. Lu, Int. J. Therm. Sci. 41 (2002) 29.
[14] P.T. Nguyen, T. Berning, N. Djilali, J. Power Sources 130 (2004) 149.
[15] J. Ihonen, Ph.D. thesis, Stockholm: Dep. of Chemical Engineering and Technology, Applied Electrochemistry, Kungliga Tekniska Hogskolan, 2003.
[16] D.J. Burford, M.M. Mench, Proceedings of the IMECE'04 ASME International Mechanical Engineering Congress and Exposition, Anaheim, CA, 2004.
[17] P.J.S. Vie, S. Kjelstrup, Electrochim. Acta 49 (2004) 1069.
[18] M. Khandelwal, M.M. Mench, J. Power Sources 161 (2006) 1106.
[19] Burheim, P.J.S. Vie, J.G. Pharoah, S. Kjelstrup, J. Power Sources, in press.
[20] C.L. Choy, K.W. Kwok, W.P. Leung, F.P. Lau, J. Polym. Sci. B: Polym. Phys. 32 (8) (1994) 1389.
[21] M. Spinnler, Int. J. Heat Mass Transfer 47 (2004) 1305.
[22] P. Zhou, C.W. Wu, J. Power Sources 170 (2007) 93.
[23] T. Hottinen, O. Himanen, S. Karvonen, I. Nitta, J. Power Sources 171 (2007) 113.
[24] Standard Test Method for Thermal Transmission Properties of Thermally Conductive Electrical Insulation Materials, ASTM Standard D-5470–06, ASTM International, Conshohocken, PA, 2007.
[25] J.R. Culham, P. Teertstra, I. Savija, M.M. Yovanovich, 8th Intersociety Conference on Thermal and Thermomechanical Phenomena in Electronic Systems, May 29–June 1, San Diego, CA, 2002.
[26] Sensor Products Inc., Madison, NJ.
[27] M. Bahrami, M.M. Yovanovich, J.R. Culham, Int. J. Heat Mass Transfer 48 (2005) 3284.
[28] I. Savija, J.R. Culham, M.M. Yovanovich, E.E. Marotta, J. Thermophys. Heat Transfer 17 (1) (2003) 43.
[29] R.J. Moffat, Exp. Therm. Fluid Sci. 1 (1988) 3.
[30] Web: http://carbon.biography.ms/.
[31] Web: http://www.boedeker.com/ptfep.htm.